Proceedings of the 17th Pan-American Conference on Soil Mechanics and Geotechnical Engineering (XVII PCSMGE), and 2nd Latin-American Regional Conference of the International Association for Engineering Geology and the Environment (IAEG), La Serena Chile, 2024.

Liquefaction behavior comparison between centrifugal tests on clean sand and silty sand

Comparación del comportamiento en estado licuado de ensayos centrífugos en arena limpia y arena limosa.

Marcelo Gonzalez

Senior Geotechnical Engineer, Independent consultant, Chile, margonza76@gmail.com

ABSTRACT: Recent failures in upstream tailing dams such as the Fundao dam, as well as the Brumadinho dam and Newcrest´s Cadia dam, have shown that non-cohesive sandy silts or silty sand have a high susceptibility to flow liquefaction. Two centrifugal tests at 25g were carried out to evaluate the response of clean sand and silty sand when liquefaction occurs. The test cases were: (1) Ottawa sand F#55 without fine particles and (2) a combination of Ottawa sand F#110 with 21% non-plastic fine particles (crushed Ottawa sand). Both tests were carried out at a similar relative density, prototype hydraulic conductivity through the use of viscous fluid and water and used the same sample preparation methodology. The results showed that both tests liquefied, but the test with the Ottawa sand without fine particles, has a failure that is mostly associated with cyclic liquefaction behavior, unlike the test with the Ottawa sand with fine particles, which has a behavior similar to that observed in the cases of flow liquefaction. The difference observed in the compressibility index of both deposits can be a Geotechnical promising laboratory parameter to help in the prediction between flow- cyclic failures behavior.

KEYWORDS: Compressibility index, Cyclic mobility, flow failure liquefaction, fine content

1 INTRODUCTION

Historical failures due to liquefaction triggered by earthquakes can be grouped mainly into two cases: (1) flow failures type, which is characterized by a spontaneous loss of resistance and uncontrolled large-magnitude deformations, and (2) cyclic mobility failure type, caused due to an accumulation of excess pore pressure during earthquakes and which is distinguished by deformations of lower magnitude (compared to the flow failures type) limited mainly to the time of earthquake occurrences. Cases of flow failures triggered by earthquakes are the Sheffield dam (1925), El Cobre tailing dam (1965) and Lower San Fernando dam (1971).

A more formal definition of flow and cyclic liquefaction is given by Roberson and Fear (1997), which define both as:

- Flow liquefaction applies to strain softening soils only and requires that in an undrained response, the in-situ shear stress component (stress larger than the K_o condition) be greater than the ultimate or quasi steady state resistance of the soil. The flow liquefaction can be triggered by either monotonic or cyclic loading and the onset of soil structural collapse is controlled by the collapse surface or low liquefaction surface (Sasitharan et. al.,1994)
- Cyclic liquefaction requires undrained cyclic loading during which shear stress reversal occurs or zero shear stress can develop, in other words when the in-situ static shear stress are low compared to the cyclic shear stresses and the addition of both components is smaller (or partially greater during the cyclic loading) than the ultimate or quasi steady state soil resistance. At zero effective stress no shear stress exists and when shear stress is applied, pore pressure drops as the material tends to dilate, but a very soft initial stress strain response can develop resulting in large deformations. This phenomena can occurs in dilative o contractive soils, the only requirement is that the cyclic loading will be sufficiently large in size and duration.

The cases of cyclic mobility when no shear stress reversal or zero effective stress develop, have not been considered in this current paper.

This research analyzes two centrifuge tests on clean Ottawa sand F55 and Ottawa sand F110 plus 21% non-plastic silt (silt created by crushed Ottawa sand), selected from a series of other centrifuge tests conducted by Gonzalez M. (2008) in order to analyze the response between clean sand and silty sand when the phenomenon of liquefied occur at similar initial prototype permeability and relative density. The liquefaction behavior is analyzed according to the definitions previously described and some conclusions in respect to the inclusion of fine particles are delineated at the end of this paper.

2 CENTRIFUGE MODEL TESTS

Two different centrifuge tests were conducted with both using different modeling philosophies in the selection of the soil and pore fluid. As shown in Figure 1, both centrifuge experiments: (i) used a laminar box inclined 2 degrees to the horizontal; (ii) filled the box with loose saturated sand; and (iii) applied the same prototype base shaking. Also, both tests were done at a centrifugal acceleration of 25g, so that the 0.24 m tall model scaled to a 6 m deep prototype deposit and were prepared by the dry pluviation method. As shown in Figure 1, the centrifuge model deposits were instrumented, so as to measure ground accelerations, pore pressures, and lateral and vertical ground displacements. The two centrifuge tests were as follows:

- Test FF-V1, which used Ottawa F#55 sand at an initial void ratio, e = 0.723, saturated with a viscous fluid 25 times the viscosity of water in order to model the prototype permeability at 1g of k = 12x10^{-3} cm/s, see Table 2. This follows the common centrifuge modeling practice at centrifuge centers around the world. The pore fluid used corresponds to a mixture of water and cellulose ether termed Methocel, which has essentially the density of water and does not significantly modify the properties of the soil (Madabhusi et al., 1994; Stewart et al., 1998)
- Test FF-P2, which used the modified Ottawa silty sand (21% fines content) of properties summarized in Table 1 and Figure.2, labeled "Scaled Sand," and saturated with water rather than viscous fluid. This Scaled Sand was obtained by mixing a finer Ottawa sand with non-plastic silt, designed to have a grain size distribution curve more or less parallel to the original prototype Ottawa F#55 sand, and having a prototype permeability at 25 g of k = 9x10^{-3} cm/s, see Table 2. This Scaled silty sand was placed very loose at an initial void ratio of e = 0.770. Assuming that the use of conventional methods as the Japanese Standard JIS A 1224:2009 for determining the maximum and minimum density are applicable for soils with non-plastic fines content greater than 5%, it can be indicated that the relative density estimated for the test was 35%.

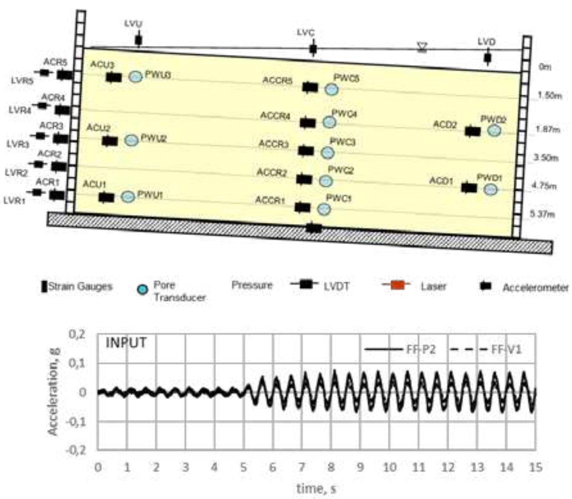

Figure 1: Setup and instrumentation of the centrifuge model tests and the base input motion

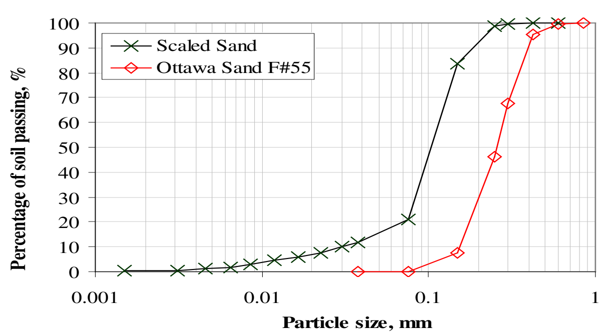

Figure 2: Grain size distributions of the two sands used in the centrifuge tests

Table 1: Soils used in full scale and centrifuge tests

Soil	D_{50} mm	D_{10} mm	Fines content, FC (%)	Minimum void ratio	Maximum void ratio	Gs
Ottawa F#55 Sand	0.258	0.155	0.1	0.61 (1)	0.80 (2)	2.67
Scaled Sand	0.103	0.031	21	0.43 (3)	0.96 (3)	2.69

Notes:
(1) Minimum Void Ratio (ASTM D4253)
(2) Maximum Void Ratio (ASTM D4254 Method C)
(3) Japanese Standard JIS A 1224:2009 Test Method

Table 2: Soil testing parameters in liquefaction/lateral spreading centrifuge tests at 25g simulating 6m thick sand deposit

Test	Void ratio	Relative density (%)	Pore fluid viscosity (cp)	Prototype saturated permeability coefficient (cm/s)	Normalized Sheer wave velocity V_{s1} (m/s)(1)	Compression index, Cc
FF-V1	0.723	40	25	12 x10^{-3}	174	6.4 x 10^{-3}
FF-P2	0.770	35	1	9 x10^{-3}	132	66 x 10^{-3}

Notes: (1) V_{s1} = shear wave velocity, V_s at a vertical effective overburden pressure, σ'_{v0} =1 atmosphere = 101.33 kPa

2.1 *Input acceleration*

The base input acceleration, plotted in Figure. 1, had a duration of 15 s and a frequency of 2 Hz, consisting of four amplitude phases and a total of about 30 sinusoidal cycles. The first 10 cycles (5s) had a very small acceleration amplitude (≈ 0.01g), designed to evaluate the dynamic response characteristics of the deposit with little or no generation of excess pore pressures and no lateral spreading.

This first phase of about 0.01 g was to be followed by a phase of 10 cycles of approximately 0.05g acceleration amplitude. The last shaking phase after 5 s was designed to progressively increase the excess pore water pressure up to liquefy the deposit and to observe the corresponding accumulative permanent lateral displacement in the downslope direction.

2.2 *Initial shear wave velocity*

The base input of first shaking phase – applied between 0 and 5 s, induced dynamic shear strains lower than 0.01% in both soil tests (Figure 8). A System Identification (SI) technique (Elgamal et al., 1995; Zeghal et al., 1995) was used to obtain the secant shear modulus from the measured stress-strain loops at various depths, and correction of this modulus to account for stress-strain nonlinearity. From the modulus, the shear wave was obtained. The results are presented in Figure. 3 together with others results from full scale and centrifuge tests using Ottawa sand but varying water and viscous as pore fluid and the sample preparation method between hydraulic and dry pluviation (Abdoun et. al. 2013). As expected for this homogeneous deposits, Vs increases with depth from very low values near the ground surface to the bottom of the models. The normalized shear wave velocities measured at 1atm corresponds to V_{s1} = 174 m/s and 132 m/s for Tests FF-V1 and FF-P2, respectively. These two values of V_{s1} have also been listed in Table 2 and are consistent with the liquefiable sand sites used by Andrus and Stokoe (2000) to develop their Vs–based liquefaction evaluation chart (Dobry 2010).

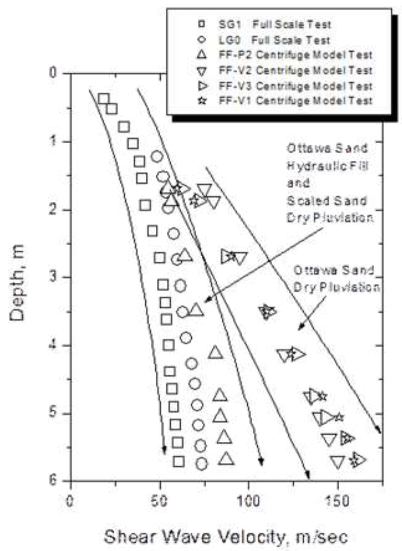

Figure 3: Shear wave velocity profiles for: (1) centrifuge tests using Ottawa sand, dry pluviation preparation and viscous fluid (FF-V1, FF-V2, FF-V3), (2) Scaled sand, water fluid and dry pluviation and (3) full-scale tests, water fluid and hydraulic fill preparation method (LG-0 and SG-1)

The values of the normalized shear waves and velocity profiles shows that the clean sand sample has a greater structure stiffness than the silty sand sample. The existence of fine on the coarse sand matrix allows the creation of soil structures with higher void content (Thevanayagam, S., et. al. 2003), which manifests itself in less rigid structures and lower shear wave velocities.

2.3 *Quasi and steady state curves*

Literature results from published triaxial tests on Ottawa sand and a series of triaxial compression tests performed in the current research under drained and undrained conditions on Ottawa F#55 and Scaled Sand were used to determine the ultimate and quasi-steady state curves for both sands. From the previous information, cero cohesion and a residual friction angle value for Ottawa sand and Scaled Sand were estimated in ϕ_u = 30° and ϕ_u = 20°, respectively. Figure 4 shows the curves for both sands in the void ratio and effective confining pressure e – p' space. In the same figure was included the range of void ratios and effective confined pressure expected to have the samples before the input shaking was applied.

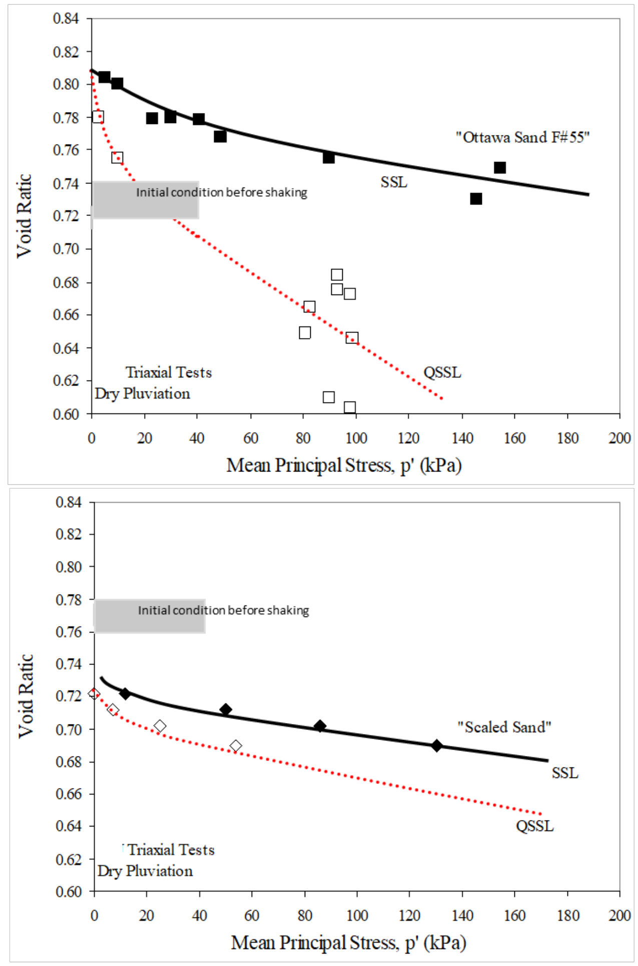

Figure 4: Quasi and steady state curves and the range of initial void ratios and effective confining pressures before shaking for: (a) Clean sand Ottawa F#55 and (b) Scaled sand (silty sand) F#110 plus 21% non- plastic silt

From Figure 4 it can be seen that the centrifugal test using clean Ottawa sand at the ranges tested of initial void ratio (before applying the earthquake) and prototype effective confinement pressures will behave mainly dilative and quasi contractive response to the failure stage. The above indicates that a sand failure due to liquefaction will most probably corresponds to a cyclic liquefaction failure type. On the other hand, the range of void ratios and prototype effective confining pressures of the Scaled Sand centrifuge test shows a response purely contractive to reach failure which predict a flow type behavior if liquefaction occur.

2.4 *Compression index*

Compressibility index from consolidation laboratory testing were available for the dry pluviated Ottawa sand and scaled sands. For the first, a value of Cc = 6.4×10^{-3} was obtained which is ten times lower than the value obtained for the scaled sand of Cc = 66×10^{-3} (Table 2).

3 RESULTS

The following paragraphs describe the results recorded by the instruments in both centrifugal tests once the dynamic load was initiated. The time histories at three representative depths of the deposit: 1.5m, 3.5m and 4.8m are described.

3.1 *Excess pore water pressure*

Figure 5 shows a comparison between the excess pore water pressure ratio measured in tests FF-V1 and FF-P2 during the shaking. As noted in the figure, both centrifugal tests do not show a significant increase in excess pore water pressure (EPWP) during the first phase of shaking with an amplitude around 0.01g (first 5s). In the case of the centrifuge test using Scaled Sand (silty sand), the EPWP has a maximum increase of $r_u = 0.30$ at the model surface, while the clean sand model has no increase in EPWP.

After, the first stage of the shaking, a gradual increase in the EPWP is observed in both centrifugal tests with the speed of the increment being greater at the surface and less at the bottom of the deposit.

Only in the centrifugal test using silty sand (FF-P2) is the liquefaction phenomenon observed at the full height of the deposit ($r_u \geq 0.9$). In the case of the test using clean sand (FF-V1), liquefaction is only observed in the first two meters of the surface.

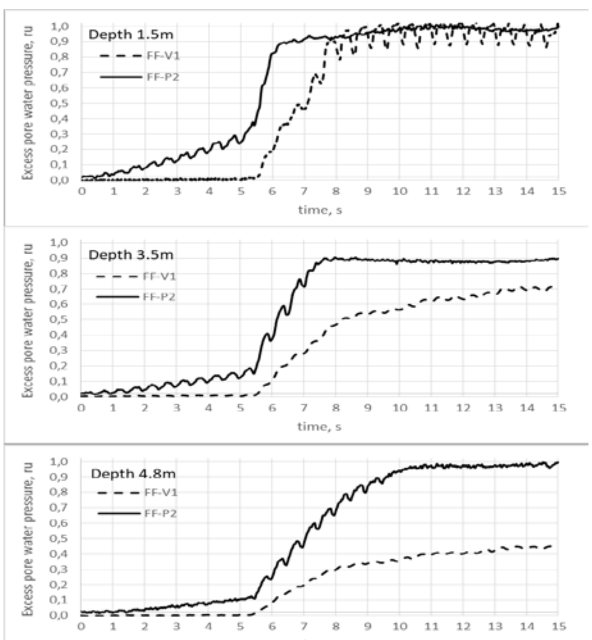

Figure 5: Excess pore water pressure ratio time history for both centrifuge tests. Clean sand (FF-V1) and Scaled sand (silty sand, FF-P2)

3.2 *Acceleration*

The acceleration on time and depth can be observed for both centrifugal tests in Figure 6. As seen in the figure, for both tests no degradation of the acceleration is observed for the first shaking phase (first 5 s), which agrees with the non-existence of excess pore pressure at that stage.

In the second shaking phase (after 5 s), a degradation of acceleration is observed in both centrifugal tests product of the increment of the excess pore pressure in the soil. In the case of the test using Scaled Sand (silty sand), none accelerations are recorded at the superficial 4m of the soil deposit, unlike the case of the clean sand test (FF-V1).

For the case of clean sand, acceleration spikes were observed at 1.5m depth which are associated with the dilation behavior of the soil as moving downslope direction.

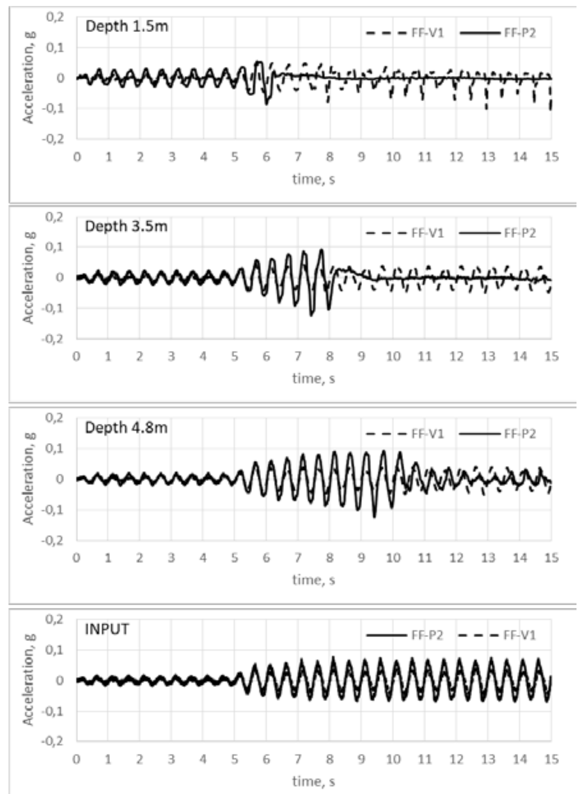

Figure 6: Acceleration time history for both centrifuge tests. Clean sand (FF-V1) and Scaled sand (silty sand, FF-P2)

3.3 *Lateral permanent displacement*

Figure 7 shows the horizontal deformation time history at different soil deposit depths. It is clear to note in the figure, that only the centrifugal test using Scaled Sand (silty sand) for the second dynamic loading phase, presents considerable horizontal deformations (compared with the clean sand deposit) as a result of the liquefaction phenomenon.

It is worth mentioning that the deformations described in Figure 7 for the FF-P2 test are limited by the capacity of the laminar container used.

The high speed of horizontal displacement, its spontaneous initiation and its uncontrollable phenomenon are characteristic of flow-type liquefaction faults.

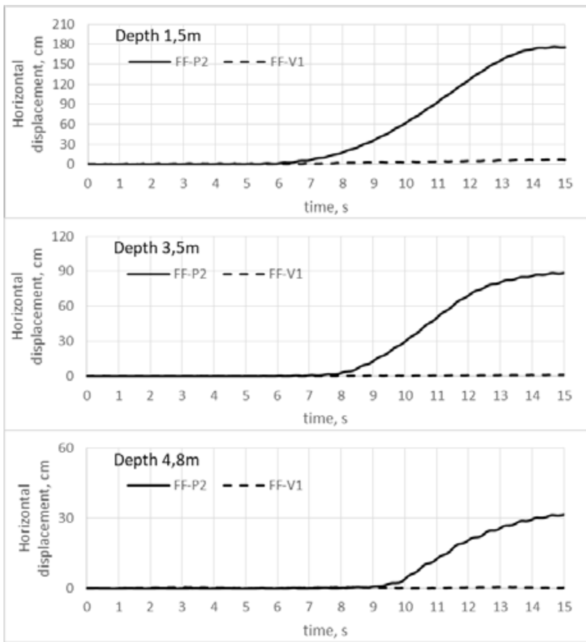

Figure 7: Horizontal displacement time history for both centrifuge tests. Clean sand (FF-V1) and Scaled sand (silty sand, FF-P2)

3.4 *Cyclic stress – strain*

Using System Identification (SI) technique, the shear stresses and strains were estimated at different soil deposit depth for both centrifugal tests.

Figure 8 shows the cyclic component of the shear stresses and strains at the depth of 1.7m from the surface for both centrifuge tests. To analyze the two shaking phases, different colors were used to describe the first 5 s and the following time.

As seen in Figure 8, for the initial shaking phase (first 5 s) no significant degradation of the shear stress is observed in both tests and maximum shear stresses around of 0.1kPa were recorded.

After the 5s of shaking, during the liquefaction condition, in both tests the shear stiffness degrade with a reduction of the cyclic shear stresses and increment of the cyclic shear strains. For the Scaled Sand (silty sand) test, the secant shear stiffness degraded up to values around to cero and shear strains close to 0.2% were observed. On the other hand, the clean sand test shows a degradation of the secant shear stiffness less critical than that observed in the Scaled Sand (silty sand) and cyclic shear strain close to 0.05% were observed.

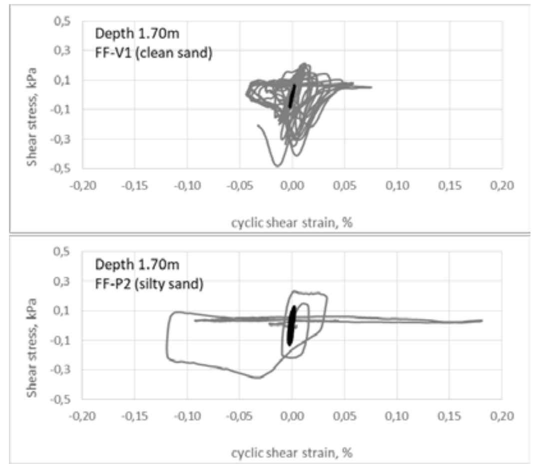

Figure 8: Cyclic shear – strain loops for the shaking duration. Black color for the first 5 s shaking time and lead color for the 5 s to 15 s. Clean sand (FF-V1) and Scaled sand (silty sand, FF-P2)

4 CONCLUSIONS

Based on the results presented in this current research, the following conclusions can be drawn:

- According to the shear wave velocities and compressibility index determined in the tested soil deposits, it is possible to indicate that at a similar relative density, the sample created by using silty sand has an initial structure (before applying the dynamic load) less stiff and more compressible than the structure that is formed by using clean sand
- Both centrifuge tests liquefied when the second shaking phase occurred. The test constructed using clean sand liquefies only at shallow depths (up to 2 m below the surface); unlike when liquefaction occurs in almost the entire soil deposit created with silty sand.
- Based on the initial condition location with respect to the steady and quasi-steady state lines of the clean sand and silty sand, plus the response of the soil in terms of acceleration, excess pore pressure and displacements, it can be said that the Silty sand deposit mainly presents a contractive behavior, unlike the clean sand that presented a dilative and contractive behavior during the shaking.
- The response observed in terms of acceleration, excess pore pressure and displacement of the silty sand deposit subjected to a dynamic load, can be associated mainly to a failure due to liquefaction of the flow type, not so for the clean sand deposit, whose response can be more associated with a liquefaction failure of the cyclic type.

5 ACKNOWLEDGEMENTS

The current research would not have been possible without the support in infrastructure and valuable comments from the research members and academics of the Civil and Environmental Engineering department_ Rensselaer Polytechnic Institute (RPI)

6 REFERENCES

Andrus, R. D. and Stokoe II, K. H., 2000. Liquefaction Resistance of Soils from Shear-Wave Velocity, J. Geotech. Geoenviron. Eng., 126(11), 1015-1025

Abdoun T., Gonzalez M., Thevanayagam S., Dobry R., Elgamal A., Zeghal M., Mercado VM., El Shamy U., 2013. Centrifuge and large-scale modeling of seismic pore pressures in sands: Cyclic strain interpretation, Journal of geotechnical and geoenvironmental engineering 139 (8), 1215-1234

Dobry, R. 2010. “Comparison between Clean Sand Liquefaction Charts Based on Penetration Resistance and Shear Wave Velocity.” Proc. 5th Intl. Conf. on Recent Advances in Geotechnical Earthquake Engineering and Soil Dynamics and Symposium in Honor of Prof. I.M. Idriss (S. Prakash, ed.), San Diego, CA, Paper No. IMI4, 6 pages

Dobry, R., Thevanayagam, S., Medina, C., Bethapusi, R., Elgamal, A., Bennett, V., Abdoun, T., Zeghal, N., El Shamy, U., and Mercado, V. M. 2010. “Mechanics of Lateral Spreading Observed in a Full-Scale Shake Test.” J. Geotechnical and Geoenvironmental Engineering, ASCE

Elgamal, A.-W., Zeghal, M., Tang, H. T., and Stepp, J. C. 1995. “Lotung Downhole Array. I: Evaluation of Site Dynamic Properties.” J. Geotech. Eng., 121(4), 350-362

Gonzalez, M., 2008. “Centrifuge Modeling of Pile Foundation Response to Liquefaction and Lateral Spreading: Study of Sand Permeability and Compressibility Effects Using Scaled Sand Technique.” PhD Thesis, Dept. of Civil and Environmental Engineering, Rensselaer Polytechnic Institute, Troy, NY

Madabhushi, S. P. G. 1994. “Effect of Pore Fluid in Dynamic Centrifuge Modeling.” Proc. Centrifuge 94 (Leung, Lee and Tan, eds.), Balkema, Rotterdam, pp. 127-132

Robertson, P. K., and Fear C.E., 1995. Liquefaction of sand and its evaluation. First International Conference Earthquake and Geotechnical Engineering, 1ICEGE, 1253 – 1289

Sasitharan, S., Robertson, P.K., Sego, D.C., and Morgenstern, N.R.1994. State boundary surface for very loose sand and its practical implications. Canadian Geotechical Journal, 31(3): 321-334

Stewart, D. P., Chen, Y. R., and Kutter, B. L. 1998. “Experience with the Use of Methylcellulose as a Viscous Pore Fluid in Centrifuge Models.” Geotechnical Testing J., ASTM, 21(4):365-369, December

Thevanayagam, S., Shenthan, T., and Kanagalingam, T. 2003. “Role of Intergranular Contacts on Mechanisms Causing Liquefaction and Slope Failures in Silty Sands.” Final Report USGS Award No. 01HQGR0032 and 99HQGR0021, US Geological Survey, Dept. of Interior, 396p

Zeghal, M., Elgamal, A.-W., Tang, H. T., and Stepp, J. C. 1995. “Lotung Downhole Array. II: Evaluation of Soil Nonlinear Properties.” J. Geotech. Eng., 121(4), 363-378

INTERNATIONAL SOCIETY FOR
SOIL MECHANICS AND
GEOTECHNICAL ENGINEERING

SIMSG ISSMGE

This paper was downloaded from the Online Library of the International Society for Soil Mechanics and Geotechnical Engineering (ISSMGE). The library is available here:

https://www.issmge.org/publications/online-library

This is an open-access database that archives thousands of papers published under the Auspices of the ISSMGE and maintained by the Innovation and Development Committee of ISSMGE.

The paper was published in the proceedings of the 17th Pan-American Conference on Soil Mechanics and Geotechnical Engineering (XVII PCSMGE) and was edited by Gonzalo Montalva, Daniel Pollak, Claudio Roman and Luis Valenzuela. The conference was held from November 12th to November 16th 2024 in Chile.